

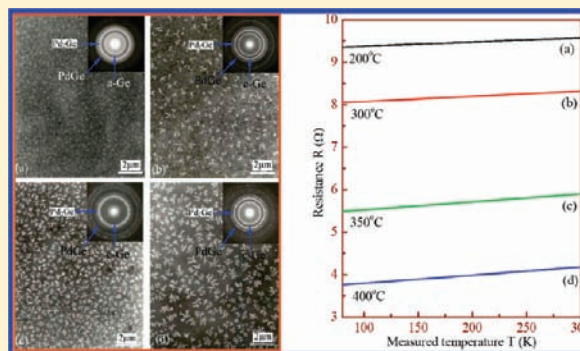
Probing into Interesting Effects of Fractal Ge Nanoclusters Induced by Pd Nanoparticles

Zhiwen Chen,^{*,†,‡} Quanbao Li,[†] Jian Wang,[†] Dengyu Pan,[†] Zheng Jiao,[†] Minghong Wu,^{*,†} Chan-Hung Shek,[‡] C. M. Lawrence Wu,[‡] and Joseph K. L. Lai[‡]

[†]Shanghai Applied Radiation Institute, Institute of Nanochemistry and Nanobiology, School of Environmental and Chemical Engineering, Shanghai University, Shanghai 200444, People's Republic of China

[‡]Department of Physics and Materials Science, City University of Hong Kong, Tat Chee Avenue, Kowloon Tong, Hong Kong

ABSTRACT: Metal/semiconductor thin films are a class of unique materials that have widespread technological applications, particularly in the field of microelectronic devices. New strategies of fractal assessment for Pd/Ge bilayer films formed at various annealing temperatures are of fundamental importance in the development of micro/nanodevices. Herein, Pd/Ge bilayer films with interesting fractal nanoclusters were successfully prepared by evaporation techniques. Temperature-dependent properties of resistance and fractal dimensions in Pd/Ge bilayer films with self-similar Ge fractal nanoclusters were investigated in detail. Experimental results indicated that the fractal crystallization behavior and film resistance in Pd/Ge bilayer films are influenced significantly by annealing temperatures and fractal dimensions. The measurements of film resistance confirmed that there is an evident relationship between the film resistance and the fractal dimension. These phenomena were reasonably explained by the random tunneling junction network mechanism.



1. INTRODUCTION

Metal/semiconductor thin films are fundamental to the development of smart and functional materials, devices, and systems.^{1–3} Considerable effort has focused on the microstructure evolution and formation mechanism of fractal architectures in nonequilibrium growth processes of materials science.^{4–6} The nonequilibrium growth of metal/semiconductor thin films during crystallization of amorphous semiconductor is a rather peculiar problem.^{7,8} There is a very sensitive and complex dependence of thin-film microstructure on growth conditions.^{9,10} It is known that lateral interdiffusion between atoms of metal and semiconductor at short range is a nonequilibrium disordered growth system, which is accompanied by crystallization of amorphous semiconductor and formation of fractal structure.^{11,12} Diffusion in disordered systems does not follow the classical laws, which describe transport in ordered crystalline media. This may lead to many anomalous physical and chemical properties.^{1,2}

In fact, the self-similar fractal structure of metal/amorphous semiconductor (M/a-S) bilayer films during annealing is essential to various physical and chemical properties.^{13,14} Due to the technological applications of metal/semiconductor bilayer films, the main advances in the understanding of these processes have come from fractal theory.¹⁵ Traditionally, the fractal growth process in disordered systems has been understood by the diffusion-limited aggregation (DLA) model.¹⁶ This model neither correlates the fractal nanoclusters with the microstructure evolution nor systematically considers the dependence of macroscopic

properties on fractal crystallization. The microstructure frequently has a profound effect on the properties of the thin-film system, e.g., magnetic, electrical, mechanical, optical, etc.^{17–24} Fractal crystallization of an amorphous semiconductor in M/a-S bilayer films during annealing is also essential to various physical and chemical properties. However, the relationship between the various properties and fractal crystallization in M/a-S bilayer films has been less studied. Usually the fractal structures can be formed in M/a-S bilayer films during crystallization of the amorphous semiconductor layer in contact with the metal layer.^{25,26} The M/a-S bilayer films after fractal crystallization are inhomogeneous. The percolating characteristics of inhomogeneous systems have been reported by Hauser and Song et al.^{27,28} Yagil et al. observed the electrical breakdown behavior of the semicontinuous Au and Ag films.²⁹ Ye et al. investigated the voltage–current ($V-I$) behavior of the Ag and Pt thin films on a ceramic substrate.² They found that the Ag or Pt thin film sputtered on ceramic substrate with the random fractal shows nonlinear $V-I$ behavior, in which dR/dI is a negative value. It is known that the fractal patterns can be easy to form under some external techniques such as annealing, agglomeration of nanoparticles, and irradiation.^{30,31} Much work has been devoted on the mechanisms of fractal formation experimentally, while little attention has been paid to elucidate the possible macroscopic properties

Received: April 18, 2011

Published: June 17, 2011

of fractal architectures such as electrical properties in these thin films.

The purpose of this paper is to characterize the dependence of resistance on fractal crystallization in Pd/Ge bilayer films induced by annealing. New strategies of fractal assessment for Pd/Ge bilayer films formed at various annealing temperatures are of fundamental importance in the development of micro/nanodevices. The Pd/Ge bilayer films with interesting fractal nanoclusters were successfully prepared by evaporation techniques. Temperature-dependent properties of resistance and fractal dimension in Pd/Ge bilayer films with self-similar fractal nanoclusters were investigated in detail. Experimental results indicated that the fractal crystallization behavior and film resistance in Pd/Ge bilayer films are influenced significantly by annealing temperatures and fractal dimensions. The measurements of film resistance confirmed that there is an evident relationship between the film resistance and the fractal dimensions. These phenomena were reasonably explained by the random tunneling junction network mechanism.

2. EXPERIMENTAL SECTION

Specimens were prepared by evaporation on a freshly cleaved NaCl (100) single-crystal substrate in vacuum with a pressure of 2.67×10^{-3} Pa at room temperature.¹² We deposited Ge at first and then Pd without breaking the vacuum (about 2.67×10^{-3} Pa) by evaporating high-purity germanium (99.9%) and palladium (99.9%) from two resistive-heated tungsten boats, viz. the bottom layer was amorphous Ge (a-Ge) and the top one was polycrystalline Pd (p-Pd). According to the evaporation equation

$$t = \frac{m}{4\pi r^2 \rho}$$

where t is the thickness of the film, m is the mass of Pd or Ge, ρ is the density of Pd or Ge, and r is the distance from the specimen to the evaporation source; here $r = 10$ cm. The thickness ratio of the p-Pd and a-Ge films was devised to be 25/50 nm. All as-deposited specimens were annealed in a vacuum of about 2.67×10^{-3} Pa at 100, 200, 300, 350, and 400 °C for 30 min. After annealing, the specimens were floated on distilled water and then placed on copper meshes to be observed with a Philips CM20 transmission electron microscope (TEM) at an acceleration voltage of 200 kV.

By such annealing, self-similar fractal structures may be formed in these bilayer films. Since the annealing temperatures can effectively control the morphology of the fractal patterns, the density of the different fractal clusters formed at a given annealing temperature is also approximately uniform at different sites of the sample. The average value of the evaluated dimension (D), obtained from different regions, can be approximately considered as the whole sample's fractal dimension. The fractal dimension for these samples was calculated by measuring the fractal dimensions of these self-similar clusters using the conventional box-counting method.^{32,33} Temperature-dependent properties of film resistance were measured in the range 80–300 K using a standard four-probe configuration and the differential technique. The whole system was automatically controlled by a computer system with precise calibration by comparison to a standard sample.

3. RESULTS AND DISCUSSION

A typical bright-field image of transmission electron microscopy (TEM) and the corresponding selected area electron diffraction (SAED) patterns (inset at the upper left-hand corner) of the morphology for the as-prepared Pd/Ge bilayer films is shown in Figure 1. As seen in the TEM bright-field image, the as-prepared

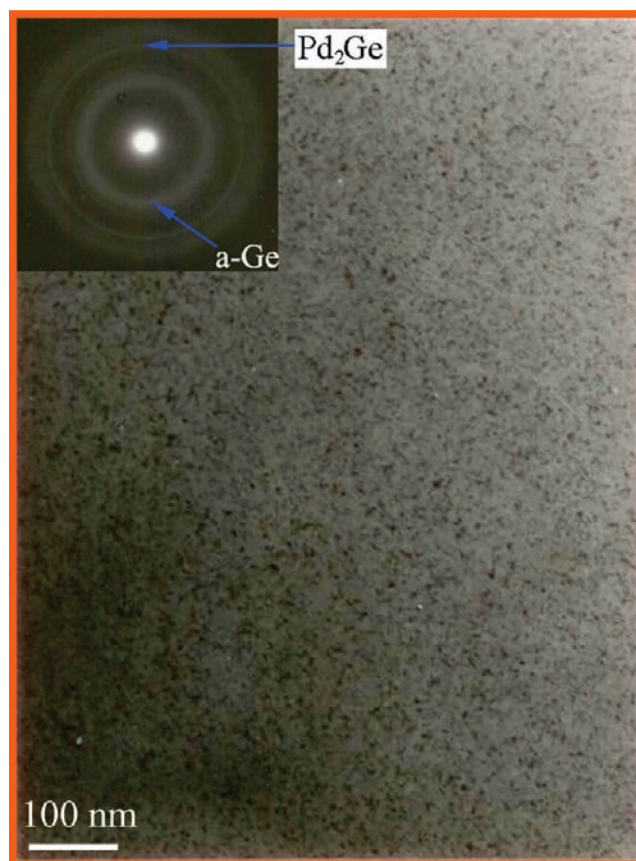


Figure 1. TEM bright-field image of the as-prepared Pd/Ge bilayer films; the inset at the upper left-hand corner shows the SAED patterns.

bilayer films are homogeneous in morphology before annealing. The nanocrystallites close to Bragg orientations were recognizable by their dark contrast. The SAED patterns (inset) for the as-prepared bilayer films confirmed that the films consist of amorphous Ge (shows a diffuse ring of a-Ge) and polycrystalline Pd (p-Pd). It can be seen that the Pd₂Ge compound is formed in as-prepared bilayer films during evaporation. This indicated that the formation process of the Pd₂Ge compound is the Pd and Ge atoms via solid-state reaction at room temperature: $2p\text{-Pd} + \text{a-Ge} \rightarrow p\text{-Pd}_2\text{Ge}$. We found that the formation temperature (room temperature) of the Pd₂Ge compound is lower than 150 °C reported by previous literature.^{34,35}

After annealing at 100 °C for 30 min, no significant structural change was caused except for a slight grain growth of the Pd and Pd₂Ge. Figure 2 shows TEM bright-field images and SAED patterns (inserted in the upper right-hand corner) of the Pd/Ge bilayer films annealed at various temperatures: Figure 2a at 200 °C, Figure 2b at 300 °C, Figure 2c at 350 °C, and Figure 2d at 400 °C for 30 min. It can be seen that the films display fractal nanoclusters at the assigned annealing temperature. The average sizes of fractal patterns are, respectively, about 210 nm (see Figure 2a), 460 nm (see Figure 2b), 680 nm (see Figure 2c), and 1.06 μm (see Figure 2d). The average sizes of fractal patterns were estimated by measuring the fractal regions. The measuring procedure is as follows: for each TEM image, we chose 10 fractal patterns at random to get an average value. The average sizes of the fractal patterns were obtained by averaging the values of TEM images with different orientations. It was found that the average sizes of

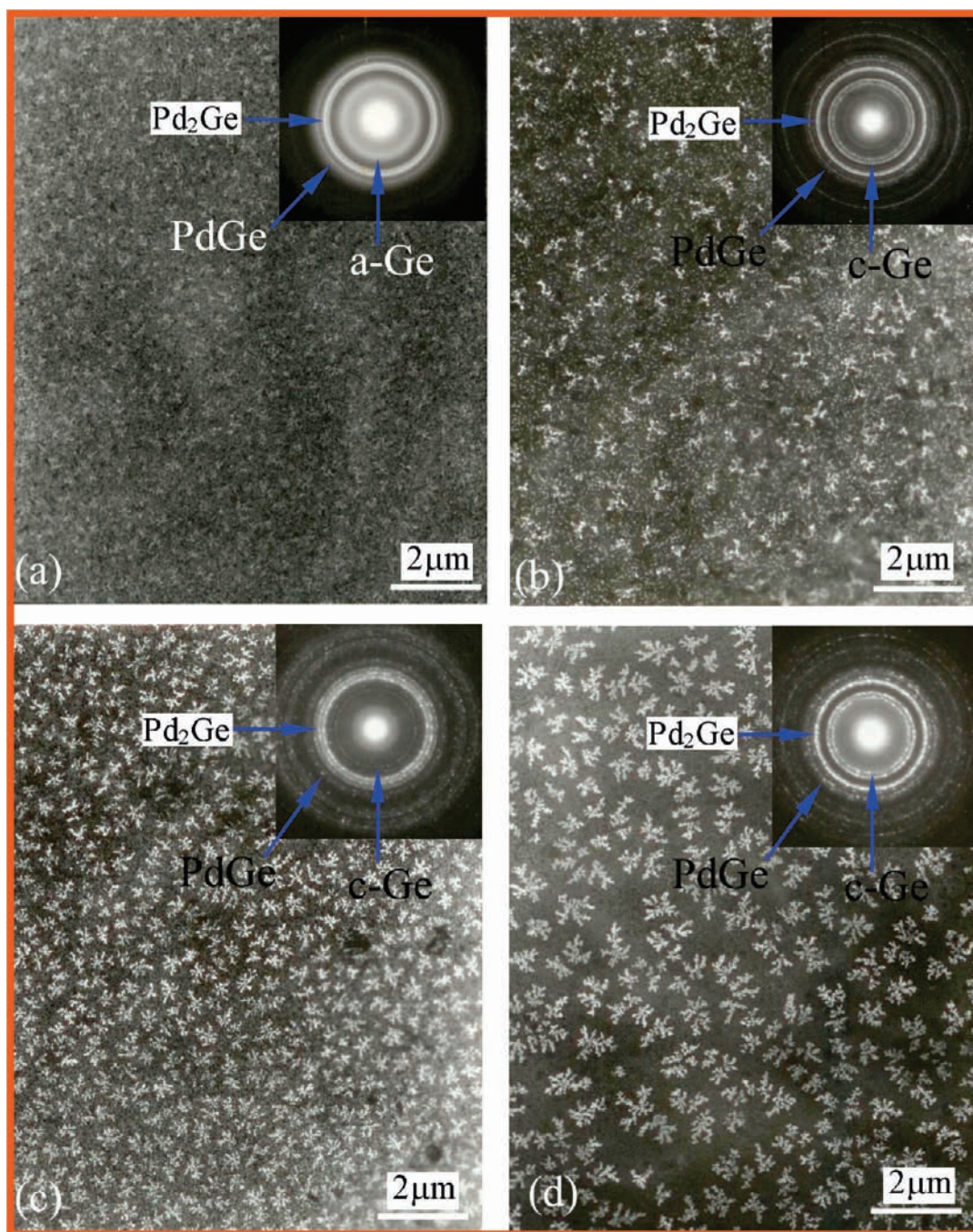


Figure 2. TEM bright-field images and SAED patterns (shown in the upper right-hand corner) of the Pd/Ge bilayer films annealed at various temperatures for 30 min at (a) 200, (b) 300, (c) 350, and (d) 400 °C.

the fractal patterns increase with increasing annealing temperature. The SAED patterns proved that, besides the Pd₂Ge compound, the PdGe compound is also formed in the assigned annealing temperature. This indicated that the Pd₂Ge compound can react completely with a-Ge and form the PdGe compound by a solid-state reaction: $p\text{-Pd}_2\text{Ge} + a\text{-Ge} \rightarrow 2p\text{-PdGe}$. After annealing at 200 °C (see Figure 2a), the diffuse ring of a-Ge was clearly visible. The fractal morphology was composed of a few thick branches, and the fractal shape was a compact structure. With increasing annealing temperature, the diffuse ring of a-Ge was replaced by nano-crystalline Ge (nc-Ge, see Figures 2b–d). When the annealing

temperature reached 400 °C (see Figure 2d), the fractal morphology composed of relatively thin branches and the fractal shape was an open structure. It is very evident that with increasing annealing temperature the fractal shape varies from compact to open and the fractal size increases.

Figure 3 shows the plots of $\ln(N)$ versus $\ln(1/L)$ of the fractal nanocluster regions in Figure 2, where L is the box size and N is the number of boxes occupied by the fractal nanoclusters. It can be seen that all plots show good linear relationship, which means that the morphologies of fractal nanoclusters have scale invariance within these ranges. Thus, these clusters can be regarded

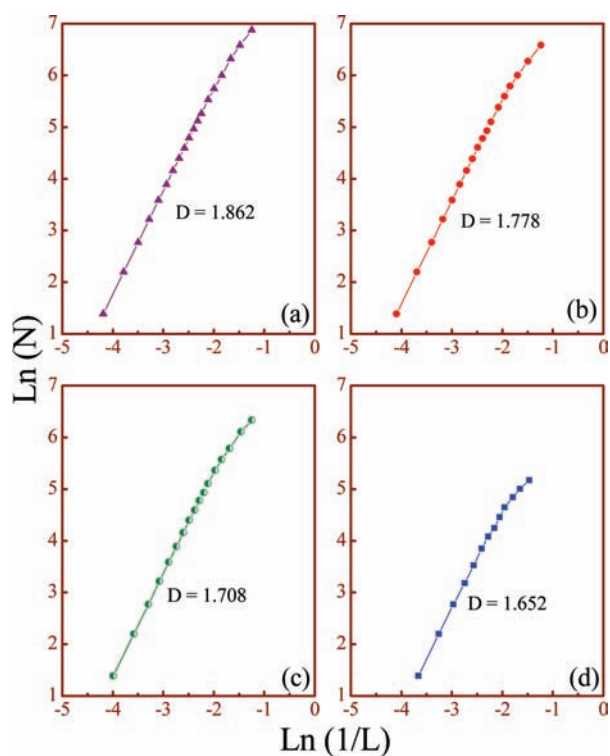


Figure 3. Plots of $\ln(N)$ versus $\ln(1/L)$ of the polycondensation fractal patterns in Figure 2, where L is the box size and N is the number of boxes occupied by the Ge fractal patterns at various temperatures for 30 min at (a) 200, (b) 300, (c) 350, and (d) 400 °C.

Table 1. Fractal Dimensions and Resistance Values of Pd/Ge Bilayer Films Annealed at Various Temperatures Measured at Room Temperature (300 K)

annealing temperature (°C)	200	300	350	400
fractal dimension	1.862	1.778	1.708	1.652
film resistance R (Ω)	9.57	8.31	5.9	4.18

as fractals. In order to obtain the fractal dimension (D), we fit a linear relationship for the function $\ln(N)$ versus $\ln(1/L)$. The results testify that the fractal dimension (D , shows in Table 1) is 1.862 at 200 °C as shown in Figure 3a, 1.778 at 300 °C as shown in Figure 3b, 1.708 at 350 °C as shown in Figure 3c, and 1.652 at 400 °C as shown in Figure 3d. It was found that the fractal dimension (D) decreases with increasing annealing temperature. The smaller fractal dimension means that the bilayer films are composed of the open and loose fractal structure with finer branches. Data analysis demonstrates that there is an obvious increase in average fractal size, and the fractal dimension generally decreases with increasing annealing temperature. In general, the fractal density is determined by the initial nucleation probability of the core nanocrystal. We found that the fractal density is calculated to be 38, 24, 31, and 12 mm^{-2} at 200, 300, 350, and 400 °C respectively. It was found that the fractal density probably tends to decrease with increasing annealing temperature. In the present work, the initial increase in nucleation probability was due to strain relaxation caused by the low short-range temperature field at 200 °C, so that the fractal density and their occupation area were

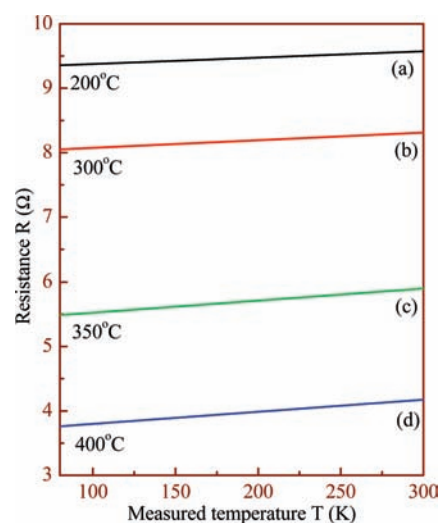


Figure 4. Film resistance values (R) versus various annealing temperatures measured from 80 to 300 K.

higher. With the increasing annealing temperature, the higher long-range temperature field may promote new nuclei and subsequent growth, which leads to fractal growth of the fine branches and lower fractal density. This fractal structure may lead to improvement in the design of micro/nanodevices for microelectronic industry applications.

At the early crystallization state of a-Ge, the crystallization energy and strain energy act together to make the Ge atoms crystallize and nucleate at some of the favorite sites at Pd/Ge and Pd₂Ge/Ge interfaces. We believe that the interdiffusion behavior between Pd and Ge atoms may influence the fractal size and dimensions. When the crystallization of a-Ge becomes easier at increasing annealing temperature, the a-Ge atoms near the grown crystal can easily coalesce onto it before the Ge grain grows further, resulting in fine branches and smaller fractal dimension. During annealing, the Ge atoms nucleate at Pd/Ge or Pd₂Ge/Ge interfaces, the surrounding Ge atoms can diffuse along the interfaces and through the Pd layer to deposit on the nucleus, and the Pd atoms can aggregate in the opposite direction. The heat released by crystallization leads to a local temperature rise in the surrounding area, and this temperature field can propagate quickly and stimulate new nuclei appearing randomly in nearby regions. The stimulated nuclei of the next generation can also cause a local temperature rise and repeat the above process many times until fractal patterns are formed. This is called the random-successive nucleation (RSN) mechanism.³⁰ In the RSN model, the experimental result of fractal dimension has been determined to be about 1.69 for annealing at 100 °C for 30 min.⁶ However, in our Pd/Ge bilayer films, the experimental results of fractal dimensions have been determined to be 1.862 and 1.778 for annealing at 200 and 300 °C for 30 min, respectively. We suggest that there may exist a significant growth behavior at the early crystallization processes of a-Ge accompanied by the RSN mechanism. The grown crystal front may cover part of the potential nucleation sites and partly prevent the nucleation process. Therefore, the random-successive nucleation and growth (RSNG) model could explain the formation processes of this fractal nanocluster.

Figure 4 shows the film resistance values (R) versus various annealing temperatures (a) 200, (b) 300, (c) 350, and (d) 400 °C

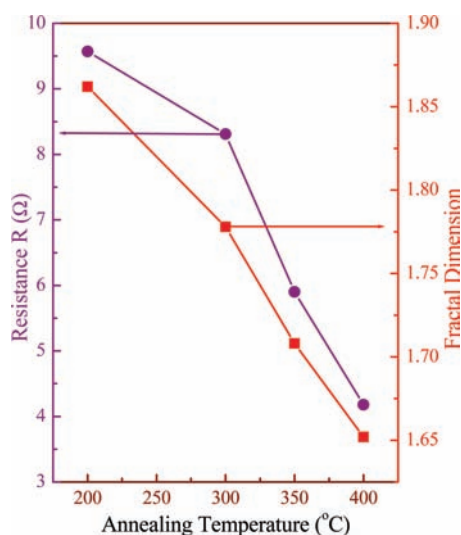


Figure 5. Film resistance values (R) versus various annealing temperatures measured at room temperature (300 K).

for 30 min measured from 80 to 300 K. It can be seen that the film resistance values of various films are evidently different. Figure 5 displays the film resistance values measured at 300 K (room temperature) for various annealing temperatures and fractal dimensions, which further exhibit this difference. Table 1 presents the fractal dimensions and resistance values of Pd/Ge bilayer films annealed at various temperatures measured at room temperature (300 K). This difference reflected that the film resistance value decreases monotonically with increasing annealing temperature and the decreasing of the fractal dimension, and the 400 °C annealing film with the lowest fractal dimension value possesses the lowest resistance value. The Pd/Ge bilayer films with interesting fractal nanoclusters are promising materials to in the future improving the design of micro/nanodevices in microelectronic industry applications.

The experimental results suggest that the film resistance R depends evidently on the fractal formation and fractal dimension in Pd/Ge bilayer films after annealing. The phenomena can be reasonably explained with the aid of the random tunneling junction network (RTJN) model.² After crystallization of a-Ge, the fractal patterns consist of the nanocrystalline Ge (nc-Ge) grains with the morphology of fine dendrite-like nanocrystals incorporating many the tunnelling junctions of varying sizes. Thus, the Pd atoms cannot constitute a homogeneous film. From the view of electrical transport, the whole thin film is made up of the linked metal islands and a series of tunnelling junctions. For the thin films annealed at various different temperatures, the sizes of the fractal branches with different fractal dimensions are different, leading to differences in the height of the potential barrier for the various tunnelling junctions, with the consequence that the breakdown voltages are also different. During measurement of the film resistance, the junction i will be in a high resistance state when the external voltage V_i is lower than the potential barrier U_i for the tunnelling junction i . In contrast, the junction i will be broken down and in a low resistance state when V_i is higher than U_i . As mentioned above, there is a relationship between the fractal dimension and the size of the fractal branches in that the number of fine branches increases with decreasing fractal dimension. Therefore, the smaller the fractal dimension, the larger the number of junctions with the smaller potential

barrier and lower resistance state. The present findings reveal new opportunities for future study of fractal architectures in metal/semiconductor thin films, with the goal of optimizing microelectronic functional material properties for specific applications.

4. CONCLUSIONS

In summary, Pd/Ge bilayer films with interesting fractal nanoclusters were successfully prepared by evaporation techniques. The experimental evidence indicates that the fractal nanoclusters with various sizes, densities, and fractal dimensions are affected by different annealing temperatures. It was found that the fractal dimension (D) decreases with increasing annealing temperature. The formation processes of Ge fractal nanoclusters can be explained by the random-successive nucleation and growth (RSNG) mechanism. The electrical properties indicate that the fractal crystallization behavior and film resistance in Pd/Ge bilayer films are influenced significantly by annealing temperatures and fractal dimensions. The film resistance R decreases monotonically with the fractal dimension. The relationship between the film resistance and the fractal dimension was reasonably explained by random tunneling junction network (RTJN) mechanism. The Pd/Ge bilayer films with interesting fractal nanoclusters are promising materials for future improvement of the design of micro/nanodevices in microelectronic industry applications.

■ AUTHOR INFORMATION

Corresponding Author

*E-mail: zwchen@shu.edu.cn (Z.C.); mhwu@staff.shu.edu.cn (M.W.).

■ ACKNOWLEDGMENT

The work described in this article was financially supported by the Shanghai Pujiang Program (10PJ1404100), Innovation Key Fund of Shanghai Municipal Education Commission (10ZZ64), National Natural Science Foundation of China (11074161, 11025526, 40830744, and 410973073), National Key Technology R&D Program in the 11th Five year Plan of China (2009BAA24B04), Shanghai Committee of Science and Technology (10JC1405400, 09530501200, 08520512200, and 09XD1401800), and Shanghai Leading Academic Discipline Project (S30109). This work was also supported by a grant from the City University of Hong Kong (Project No. 7002295).

■ REFERENCES

- (1) Tian, M. L.; Chen, L.; Zhang, S. Y.; Tan, S.; Jia, Y. B.; Hou, J. G.; Zhang, Y. H. *Phys. Rev. B* **1999**, *60*, 16078.
- (2) Ye, G. X.; Wang, J. S.; Xu, Y. Q.; Jiao, Z. K.; Zhang, Q. R. *Phys. Rev. B* **1994**, *50*, 13163.
- (3) Chen, Z. W.; Zhang, S. Y.; Tan, S.; Hou, J. G.; Zhang, Y. H.; Sekine, H. J. *Appl. Phys.* **2001**, *89*, 783.
- (4) Chen, Z. W.; Wang, X. P.; Tan, S.; Zhang, S. Y.; Hou, J. G.; Wu, Z. Q. *Phys. Rev. B* **2001**, *63*, 165413–1.
- (5) Zhang, S. Y.; Wang, X. P.; Chen, Z. W.; Wu, Z. Q.; Jin-Phillipp, N. Y.; Kelsch, M.; Phillipp, F. *Phys. Rev. B* **1999**, *60*, 5904.
- (6) Hou, J. G.; Wu, Z. Q. *Phys. Rev. B* **1989**, *40*, 1008.
- (7) Yagill, Y.; Deutscher, G.; Bergman, D. *Phys. Rev. Lett.* **1992**, *69*, 1423.
- (8) Konno, T. J.; Sinclair, R. *Philos. Mag. B* **1995**, *71*, 179.

- (9) Bosnell, J. R.; Voisey, U. C. *Thin Solid Films* **1970**, *6*, 161.
- (10) Oki, F.; Ogawa, Y.; Fujika, Y. *Jpn. J. Appl. Phys.* **1969**, *8*, 1056.
- (11) Chen, Z. W.; Zhang, S. Y.; Tan, S.; Hou, J. G.; Wu, Z. Q. *Appl. Phys. A: Mater. Sci. Process* **2004**, *78*, 603.
- (12) Chen, Z. W.; Zhang, S. Y.; Tan, S.; Hou, J. G.; Zhang, Y. H. *J. Vac. Sci. Technol. A* **1998**, *16*, 2292.
- (13) Chen, Z. W.; Zhang, S. Y.; Tan, S.; Hou, J. G.; Zhang, Y. H. *Thin Solid Films* **1998**, *322*, 194.
- (14) Chen, Z. W.; Lai, J. K. L.; Shek, C. H. *J. Phys. D: Appl. Phys.* **2006**, *39*, 4544.
- (15) Feder, J. *Fractal*; Plenum: New York, 1988.
- (16) Witten, T. A.; Sander, L. M. *Phys. Rev. Lett.* **1981**, *47*, 1400.
- (17) Chevrier, J.; Thanh, V. L. *Europhys. Lett.* **1991**, *16*, 737.
- (18) Alexander, S.; Bruinsma, R.; Hilfer, R.; Deutscher, G.; Lereah, Y. *Phys. Rev. Lett.* **1988**, *60*, 1514.
- (19) Krim, J.; Heyvaert, I.; Haesendonck, C. V.; Bruynseraede, Y. *Phys. Rev. Lett.* **1993**, *70*, 57.
- (20) Wang, S.; Halevi, P. *Phys. Rev. B* **1993**, *47*, 10815.
- (21) Madam, A. Shaw, M. P. *The Physics and Application of Amorphous Semiconductors*; Academic: New York, 1988.
- (22) Robinson, G. Y. *Thin Solid Films* **1980**, *72*, 129.
- (23) Tsai, C. C.; Nemanich, R. J.; Thomdson, M. J. *J. Vac. Sci. Technol.* **1982**, *21*, 632.
- (24) Ye, G. X.; Xu, Y. Q.; Wang, J. S.; Jiao, Z. K.; Zhang, Q. R. *Phys. Rev. B* **1994**, *49*, 3020.
- (25) Deutscher, G.; Lereah, Y. *Phys. Rev. Lett.* **1988**, *60*, 1510.
- (26) Li, B. Q.; Zheng, B.; Zhang, S. Y.; Wu, Z. Q. *Phys. Rev. B* **1993**, *47*, 3638.
- (27) Song, Y.; Lee, S.; Gaines, J. *Phys. Rev. B* **1992**, *46*, 14.
- (28) Hauser, J. J. *Phys. Rev. B* **1979**, *7*, 4099.
- (29) Yagil, Y.; Deutscher, G.; Bergman, D. J. *Phys. Rev. Lett.* **1992**, *69*, 1423.
- (30) Wu, Z. Q.; Li, L. B. *Phys. Rev. E* **1995**, *51*, R16–R19.
- (31) Chen, Z. W.; Lai, J. K. L.; Shek, C. H.; Chen, H. D. *J. Phys. D: Appl. Phys.* **2004**, *37*, 2726.
- (32) Chen, Z. W.; Zhang, S. Y.; Tan, S.; Hou, J. G. *Mater. Res. Bull.* **2002**, *37*, 825.
- (33) Forrest, S. R.; Witten, T. A. *J. Phys. A* **1979**, *12*, L109.
- (34) Wittmer, M.; Nicolet, M. A.; Mayer, J. W. *Thin Solid Films* **1977**, *42*, 51.
- (35) Hutchins, G. A.; Shepela, A. *Thin Solid Films* **1973**, *18*, 343.